Energy Conversion and Management 277 (2023) 116637

Contents lists available at ScienceDirect

Energy Conversion and Management

journal homepage: www.elsevier.com/locate/enconman

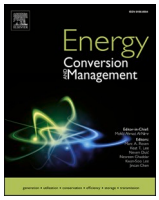

Performance comparison and suitable climatic zones of three water-mediated evaporative cooling technologies

Yang Jing, Xiaoyun Xie *, Yi Jiang

Building Energy Research Center, Tsinghua University, Beijing 100084, People's Republic of China

ARTICLE INFO

Keywords:
Indirect evaporative cooling
Theoretical model
Water-mediated
Dew point
Climatic condition

ABSTRACT

Evaporative cooling is an alternative cooling technology to conventional vapor-compression systems with lower energy use and pollution emissions. This paper presents theoretical performance comparison for three water-mediated evaporative coolers and provides a design guideline for choosing evaporative coolers under specific climates and operating boundary conditions. Theoretical solutions of counter-flow evaporative cooling are given and verified with maximum absolute and relative errors of 0.26 K and 1.23% respectively. The heat transfer coefficient of the combined heat and mass transfer is 2.72–4.95 times than the pure heat transfer process if there were no mass transfer. Climatic dividing lines of various technologies are affected by the design parameters of the system, dropping the psychrometric chart into different applicable climatic areas. The simulation results show that the climatic areas in psychometrics where indirect outperforms direct evaporative cooling will expand when increasing the air–water ratio and heat transfer coefficient, and climatic area of series indirect evaporative cooling shrinks when increasing temperature difference. The simplified selection method using such difference in merits is verified by case study, which can serve as a useful guideline for choosing the proper evaporative cooling technology for a wide range of geographical locations.

1. Introduction

With the growth of urbanization and human living standards, energy consumption and CO_2 emissions in the building sector continue to increase. As of 2018, the building sector already accounts for one-third of annual total energy consumption and 30% of total CO_2 emissions in the end-use sector[1]. The growing demand for thermal comfort promotes the rapid spread of heating, ventilating, and air condition systems (HVAC) in buildings[2], which make up approximately 50% of building energy consumption and 20% of total consumption in the USA[3]. Cooling systems are one of the most substantial energy-draining facilities in data centers, and reducing energy consumption for cooling systems is the key issue for the sustainable development of data centers[4].

Evaporative cooling technologies are used as pre-cooling or cooling devices to release waste heat into the environment. Compared with the vapor compression chiller, evaporative cooling technology has some principal advantages, such as substantial energy and cost savings, life-cycle cost effectiveness, improved indoor air quality, reduced pollution emissions, and no use of chlorofluorocarbons[5]. Evaporative cooling as a pre-cooling unit for a mechanical refrigerator reduced about 75% cooling load and 55% power consumption[6]. Using evaporative cooling instead of mechanical refrigerators can reduce about 80% of energy consumption in a fresh air conditioning application[7].

Evaporative cooling can be divided into air-mediated and water-mediated according to different mediums used to transfer cooling capacity[8]. Air-mediated evaporative cooling is usually applied in small-scale buildings such as residential and office buildings. The common air-mediated evaporative cooling structures include direct evaporative cooling (DEC)[9], indirect evaporative cooling (IEC)[10], regenerative or dew-point evaporative cooling[11], Maisotsenko cycle[12], multi-stage evaporative cooling[13], and desiccant arrangements[14]. Water-mediated evaporative cooling technologies wildly applied in large-scale centralized cooling stations are direct evaporative cooling[15], series indirect evaporative cooling[16], and parallel indirect evaporative cooling[17].

Experimental and simulated research on the cooling performance of these air-mediated and water-mediated evaporative cooling processes has been reported in recent years. Air-mediated and water-mediated direct evaporative cooling studies mainly focused on heat and mass transfer performance of different padding materials, such as about 95% of 75.37% wet-bulb efficiency of aspen fibers, 73.06% of khus fibers,

* Corresponding author.
E-mail address: xiexiaoyun@tsinghua.edu.cn (X. Xie).

https://doi.org/10.1016/j.enconman.2022.116637
Received 21 September 2022; Received in revised form 4 December 2022; Accepted 27 December 2022
Available online 5 January 2023

Nomenclature

Symbols

A	transfer area (m^2)
c_{pa}	specific heat of air (kJ/(kg·K))
c_{pea}	equivalent specific heat of air (kJ/(kg·K))
c_{pw}	specific heat of water (kJ/(kg·K))
COP	coefficient of performance
DEC	direct evaporative cooling
DT, $\triangle T$	temperature difference (K)
G_a	inlet ambient air mass flow rate (kg/s)
G_w	inlet water mass flow rate (kg/s)
h	specific enthalpy (kJ/kg)
H	time (h)
$HVAC$	heating, ventilating and air condition
IEC	indirect evaporative cooling
KA	heat transfer coefficient (kW/ K)
k_d	mass transfer coefficient of padding (kg/(m^2·s))
k_L	heat transfer coefficient of SHE (kW/(m^2·K))
k_s	heat transfer coefficient of padding (kW/(m^2·K))
m	heat capacity ratio of padding
n	heat capacity ratio of sensible heat exchanger
NTU	the number of transfer units
P	pressure (Pa)
Q	cooling capacity (kW)
r_0	latent heat of vaporization of water (kJ/kg)
RH	relative humidity (-)
SHE	sensible heat exchanger
t	temperature (℃)

Greek symbols

ω	humidity ratio (g/kg dry air)

Subscripts

a	air
db	dry-bulb
dp	dew-point
in	inlet
out	outlet
$p, pad, 2,$	padding
s	series
sat	saturated condition
$SHE,1$	sensible heat exchanger
w	water
wb	wet-bulb

78.60% of coconut fibers, and 83.89% wet-bulb efficiency of palash fibers[18]. Khalajzadeh et al.[19] presented a hybrid system combined ground heat exchanger and air-mediated classic indirect evaporative cooler, wet-bulb efficiency of which is 104%. A novel air-mediated dew-point evaporative cooling system was established to provide cooling for fresh air conditioning applications, which had a wet-bulb efficiency of 92 ~ 114% and a dew-point efficiency of 58 ~ 84%[20]. Khalid et al.[21] reported an air-mediated cross-flow Maisotsenko cycle evaporative cooler, the wet-bulb and dew-point efficiency of which varied in the range of 92 ~ 120% and 62 ~ 85%.. Some other researchers have optimized the structure and size of evaporative cooling devices.[22] The coefficient of performance (COP, cooling energy room obtained divided by electricity consumption of the indirect evaporative chiller and the fresh air handing unit) can be dramatically enhanced by 36–92% via robust optimization of supply air velocity and working air ratio.[23] Badiei et al.[24] presented a whole building energy modeling work incorporating a dew point evaporative cooler, the highest dew-point efficiency and COP of which are 0.87 and 51.1. Chen et al.[25] proposed a hybrid system combining an indirect evaporative cooler and humidification-dehumidification desalination cycle for simultaneous production of cooling and freshwater, the simulated results showed that the freshwater productivity and gain-output ratio are 25–125 L/h and 1.6–2.5.

Water-mediated indirect evaporative cooling has been widely applied in large-scale centralized cooling stations such as cooling towers, but few studies on water-mediated evaporative cooling are available. Xie and Jiang[17] introduced the water-mediated parallel IEC with a dew-point efficiency of 0.4 ~ 0.8 and a COP of 9.1. A wet-bulb efficiency of above 106% was obtained in a water-mediated series IEC experimental unit in previous work[16] Engineers cannot directly compare the wet-bulb or dew-point efficiencies reported in various pieces of research to determine which evaporative cooling technology performs better, because the cities, cooling system requirements, meteorological conditions, and designed parameters used in each research vary.

The choice of the cooling medium is determined by building type and cooling system requirements, while an appropriate evaporative cooling process should be selected according to the performance comparison of different processes under the same conditions. The wet-bulb efficiency of regenerative IEC is significantly higher than that of classic IEC in the literature[26] in Tehran, but their cooling capacity is different. Shirmohammadi et al.[27] compared the cooling performance of six classic IEC and three DEC processes, with cross-flow IEC having the highest efficiency. Farmahini-Farahani et al.[28] presented experimental investigations on the air-mediated direct, indirect, and two-stage indirect/direct evaporative cooling for six cities in Iran. Furthermore, DEC works best in temperate and dry regions, the IEC is more efficient in a hot and dry climate, and the IEC/DEC is a better choice for hot and semi-humid regions. Although this research considered the influence of meteorological conditions, it is not universal for only referring to certain designed parameters in six cities. Previous work[16] similarly compared water-mediated DEC and series IEC and showed that the DEC was more efficient in humid regions and the series IEC was suitable for dry climates, but no detailed climate ranges were given to guide the selection of appropriate evaporative cooling technologies. Many works of literature only focus on wet-bulb, dew-point, energy, or exergy efficiency and do not comprehensively consider the efficiency and cooling capacity under different climatic conditions, which is not completely fair to compare different cooling technologies. Moreover, conclusions are often limited to a specific system design and meteorological parameters, and engineers cannot easily apply these conclusions to other scenarios.

The rise of cooling systems such as data centers has expanded the application of evaporative cooling, which makes it more difficult to choose the appropriate process. In this paper, the performance of water-mediated evaporative cooling is compared under different system designed and meteorological parameters, and application ranges of different processes are given through theoretical analysis and simulation. Theoretical solutions of counter-flow evaporative cooling are given to simplify simulated mode. The clear climatic dividing lines of various evaporative cooling technologies are proposed by theoretical and simulated model, falling psychrometric chart into different applicable regions. The variations of performance partitions on the psychrometric chart is proposed to clearly reflect the applied climatic range of different processes under various design parameters. A case study illustrates how to use performance partitions of different evaporative cooling to select the appropriate process in different conditions and requirements.

2. Process description

The common water-mediated evaporative cooling technology is divided into direct evaporative cooling (DEC) and indirect evaporative cooling (IEC). The core component of direct evaporative cooling includes padding, fan, nozzles, and water collector, as shown in Fig. 1(a). The main occurrence of padding is a heat and mass transfer process with direct contact. Outdoor ambient air (state O) and returning cooling

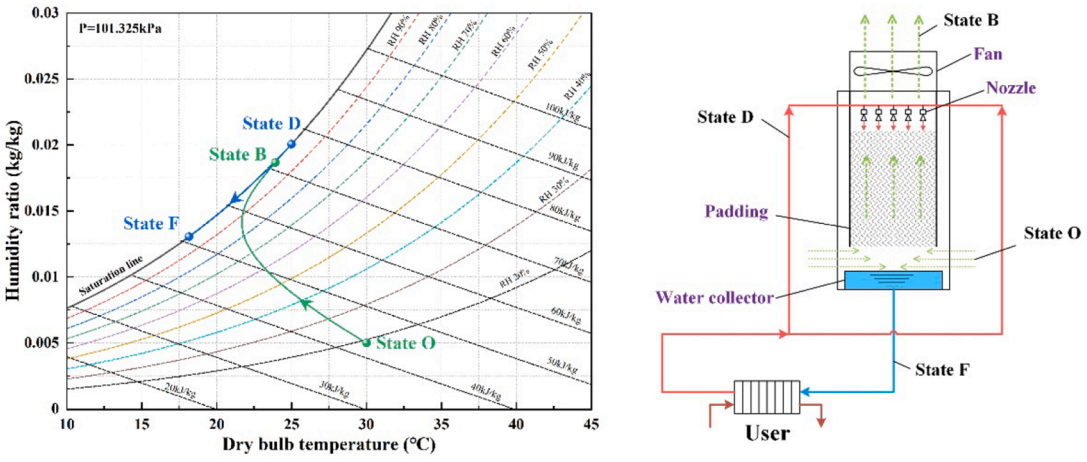

(a) Direct evaporative chillers (DEC)

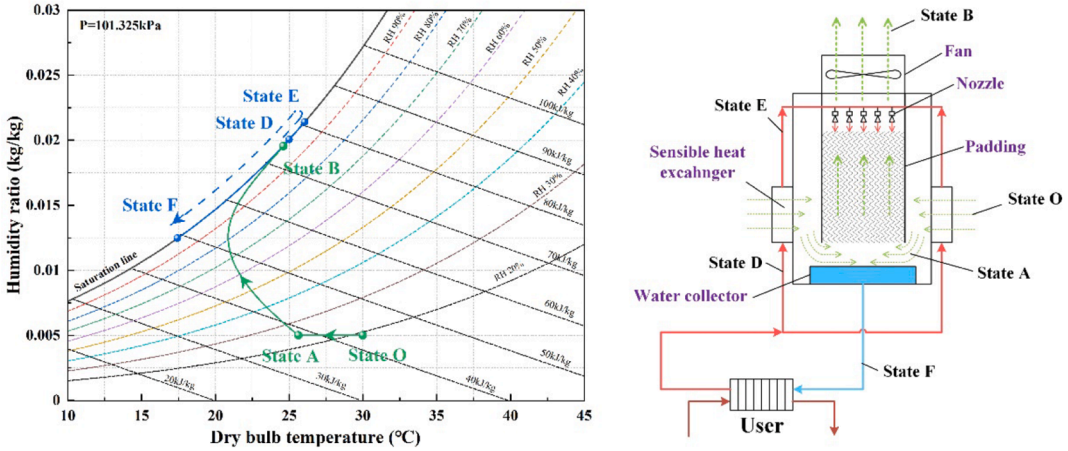

(b) Series indirect evaporative chillers (series IEC)

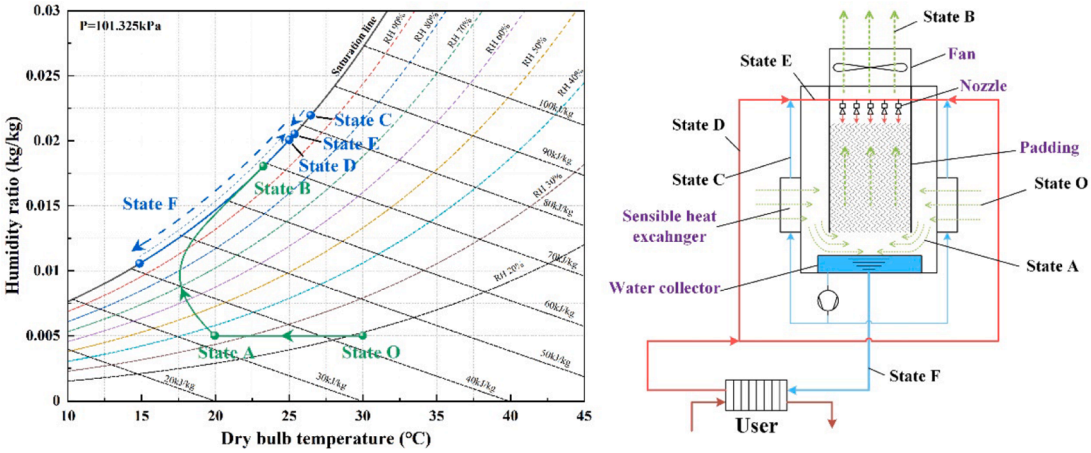

(c) Parallel indirect evaporative chillers (parallel IEC)

Fig. 1. Schematic diagrams and psychrometric charts of water-mediated evaporative chillers.

water (state D) are supplied to the padding to produce low-temperature cooling water (state F). Series and parallel connections are the two most popular indirect evaporative cooling processes, shown in Fig. 1(b) and (c). Indirect evaporative cooling processes add sensible heat exchangers (SHE) to pre-cool the outdoor ambient air based on direct evaporative cooling. Series IEC uses returning cooling water to pre-cool ambient air, while parallel IEC uses produced cooling water to pre-cool the air. State E and state A indicate the inlet water and air of padding of indirect evaporative cooling, and there is a mixing process between returning cooling water (state D) and outlet water of SHE (state C) for parallel IEC.

The three evaporative cooling processes are represented in the psychrometric chart in Fig. 1. Sensible heat exchangers cool the inlet

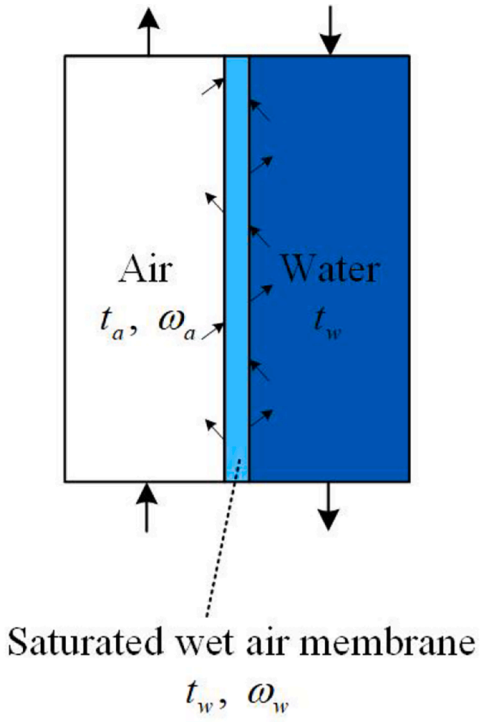

(a) Heat and mass transfer two-film model.

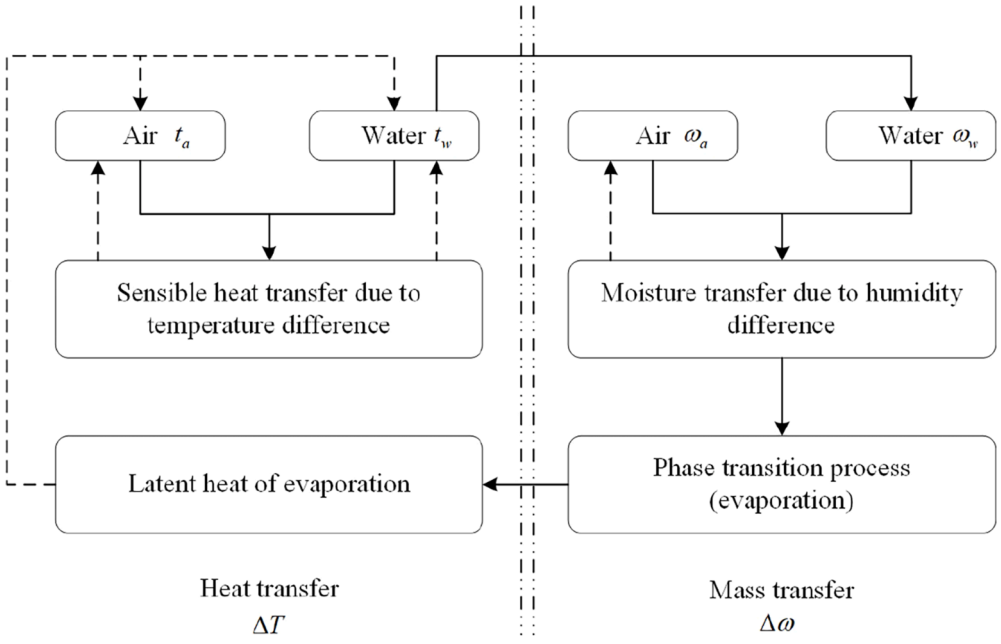

(b) Coupling effect of heat and mass transfer process.

Fig. 2. Theoretical model of heat and mass transfer process of padding.

ambient air, lowering its wet-bulb temperature, which increases the heat and mass transfer drive in the padding. Sensible heat exchangers give indirect evaporative cooling greater cooling potential but require more heat transfer for the same cooling capacity. Therefore, for series and parallel indirect evaporative cooling processes, more heat transfer area and inlet air flow rate are necessary to obtain lower output water temperature. The theoretical minimum output water temperature for direct evaporative cooling is the inlet ambient air wet-bulb temperature, while the theoretical minimum output water temperature for indirect evaporative cooling is the dew-point temperature.

3. Theoretical analysis

How to accurately predict the performance and choose the appropriate evaporative cooling process has become the most important problem in its application. In this section, analytical solutions of direct evaporative cooling and sensible heat transfer processes are given through theoretical analysis, and the theoretical performance boundary between DEC and series IEC is obtained.

3.1. Establishment of the theoretical model

The heat and mass transfer process of direct contact is the main physical phenomenon occurring in padding. Sensible heat transfer occurs when there is a temperature difference between air and water, and moisture transfer occurs when the steam partial pressure in the air and the saturated wet air membrane are different. And with the moisture transfer, the phase transition process of water evaporation will occur at the interface. The temperature and partial pressure of the saturated wet air membrane are equal to that of the water surface. The schematic diagram of the two-film theoretical model of the heat and mass transfer process is represented in Fig. 2(a).

Heat transfer, mass transfer, and phase transition processes occur simultaneously and interact with each other. The sensible heat transfer process affects the water and air temperature, and changes in water temperature lead to the different steam partial pressure of saturated wet air membrane, which in turn affects the mass transfer driving force. The mass transfer process is accompanied by a phase transition process that influences the temperature of air and water, affecting sensible heat transfer. To simplify the theoretical model of counterflow heat and mass transfer, the following assumptions are made.

(1) The constant Lewis's factor is equal to 1[29].
(2) The latent heat of evaporation is provided by water[30].
(3) The dry-bulb temperature of saturated wet air is linearly related to humidity[31].

For the counterflow heat and moisture exchange process between air and water, with the water flow in the positive direction, the theoretical model in Fig. 2 can be expressed as follows. Eq. (1) represents the air-side energy balance equation, where the change in air temperature is due to sensible heat transfer. Eq. (2) is the air-side moisture conservation equation, related to the humidity difference between the saturated wet air membrane in the water surface and the air. And based on the assumption (2), Eq. (3) represents the water-side energy balance, the water temperature change is the joint action of heat transfer and phase transition process.

$$G_a \cdot c_{pa} \cdot dt_a = -k_s \cdot dA_p \cdot (t_w - t_a) \tag{1}$$

$$G_a \cdot d\omega_a = -k_d \cdot dA_p \cdot (\omega_w - \omega_a) \tag{2}$$

$$G_w \cdot c_{pw} \cdot dt_w = -k_s \cdot dA_p \cdot (t_w - t_a) - r_0 \cdot k_d \cdot dA_p \cdot (\omega_w - \omega_a) \tag{3}$$

Where G_a and G_w represent the mass flow rate of air and water; k_s and k_d are the heat and mass transfer coefficients of the padding; r_0 is the latent heat of evaporation of water. t_a and ω_a are the dry-bulb temperature and humidity of air, and t_w and ω_w are the water temperature and saturated humidity. c_{pa} and c_{pw} denote the specific heat capacity of air and water, and A_p is the heat and mass transfer area.

Lewis factor gives an indication of relative rates of heat and mass transfer in an evaporative process. An analysis by Feltzin and Benton [32] indicated that for counterflow cooling towers a Lewis factor of 1.25 was more appropriate, while Sutherland [33] used a Lewis factor of 0.9. Lewis factor is taken to be unity so that the mass transfer coefficient is computed from the known heat transfer coefficient in this mode, which can be expressed by Eq. (4). The enthalpy of wet air is related to the dry-bulb temperature and humidity. Eq. (5) is the enthalpy of air, and Eq. (6) is the enthalpy of saturated wet air membrane on the water surface.

$$Le = \frac{k_s}{c_{pa} \cdot k_d} = 1 \tag{4}$$

$$h_a = c_{pa} \cdot t_a + r_0 \cdot \omega_a \tag{5}$$

$$h_w = c_{pa} \cdot t_w + r_0 \cdot \omega_w \tag{6}$$

For the evaporative cooling operating meteorological conditions, the humidity of saturated wet air is approximately linear with the dry bulb temperature, as shown in assumption (3). Then the enthalpy of air at the saturation line can be expressed by Eq. (8), from which a new equivalent air specific heat capacity cp_{ea} in Eq. (9) can be defined.

$$\omega_{sat} = a \cdot t_{sat} + b \tag{7}$$

$$h_{sat} = c_{pa} \cdot t_{sat} + r_0 \cdot \omega_{sat} = (c_{pa} + r_0 \cdot a) \cdot t_{sat} + r_0 \cdot b \tag{8}$$

$$c_{pea} = c_{pa} + r_0 \cdot a = c_{pa} + r_0 \frac{\Delta \omega_{sat}}{\Delta t_{sat}} = \frac{dh_{sat}}{dt_{sat}} \tag{9}$$

$$h_a = h_{sat} = h_{wb,a} = c_{pea} \cdot t_{wb,a} + r_0 \cdot b \tag{10}$$

$$h_w = c_{pea} \cdot t_w + r_0 \cdot b \tag{11}$$

Where a and b are constants relative to the defined air specific heat capacity, and $t_{wb,a}$ is the air wet-bulb temperature. Substituting Eq. (5), (6), (10), and (11) into Eq. (1), (2) and (3), the differential equations can be obtained as (12) and (13). Referring to assumptions (1) and (3), the heat and mass transfer process in direct evaporative cooling in padding is simplified as a sensible heat transfer process between air wet-bulb temperature and water temperature. Compared with Eq. (3), the existence of the mass transfer process strengthens the sensible heat transfer in Eq. (13), which is equivalent to increasing the sensible heat transfer coefficient to cp_{ea}/cp_a times of the original.

$$G_a \cdot c_{pea} \cdot dt_{wb,a} = G_w \cdot c_{pw} \cdot dt_w \tag{12}$$

$$G_w \cdot c_{pw} \cdot dt_w = \frac{c_{pea}}{c_{pa}} k_s \cdot dA_p \cdot (t_{wb,a} - t_w) \tag{13}$$

Fig. 3 shows the variation of the air equivalent specific heat capacity with different air wet-bulb temperatures. As the outdoor wet-bulb temperature increases, the air equivalent specific heat capacity increases rapidly, while the specific heat capacity of water is substantially unchanged. Therefore, under the same air–water ratio, the cooling potential of water-mediated evaporative cooling processes at high air wet-bulb temperature is significantly greater than that at low wet-bulb temperature. In the common operating range of evaporative cooling, the equivalent specific heat capacity varies from 2.79 to 5.22 kJ/kg/K, and variations of cp_{ea}/cp_a and cp_{ea}/cp_w are 2.72 ~ 4.95 and 0.67 ~ 1.25. When designing evaporative cooling air and water mass flow rates, it is necessary to fully consider the variation range of air wet-bulb temperature during operation. In most cases, the designed air mass flow rate is greater than the water flow rate, and the recommended design value of the air–water ratio of water-mediated evaporative cooling is 1 ~ 1.6. In the process of evaporative cooling, the air wet-bulb temperature varies

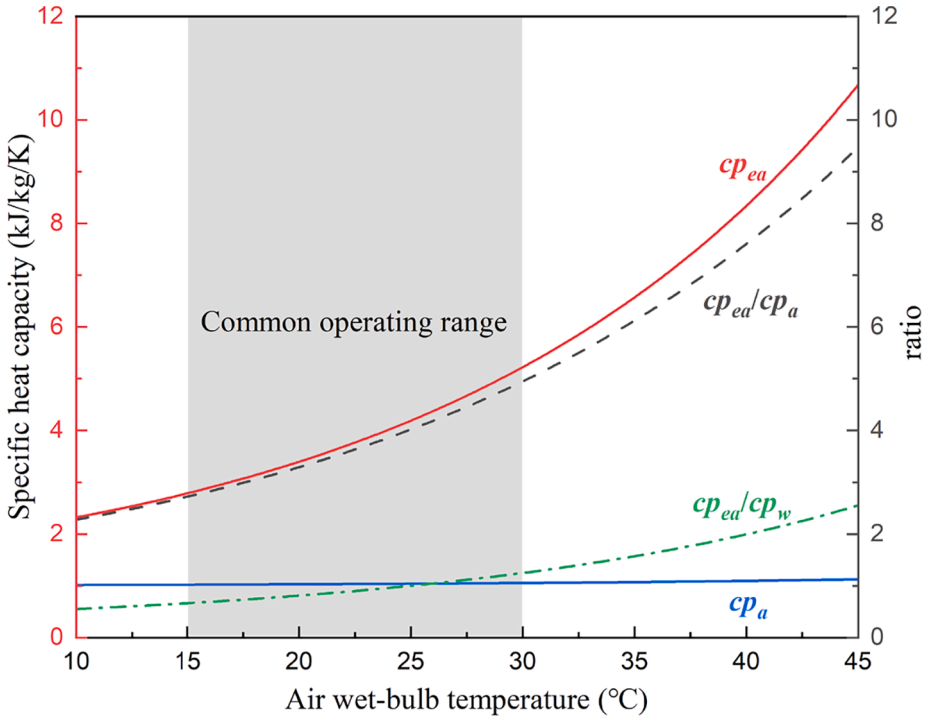

Fig. 3. The equivalent specific heat capacity versus air wet-bulb temperatures.

within a small range, and its equivalent specific heat capacity is considered to remain unchanged in the theoretical analysis according to assumption (3).

3.2. Analytical solutions and verification

The analytical solution of output water temperature of the water-mediated direct evaporative cooling can be obtained according to the differential equations of Eq. (12) and (13), and the result is shown in Eq. (14). Where $t_{w,in,pad}$ represents the inlet water temperature, and $t_{wb,a,in,pad}$ is the inlet air wet-bulb temperature. When the air flow rate, water flow rate and heat transfer coefficient of evaporative cooling are unchanged, the output water temperature is only related to the inlet air wet-bulb temperature and inlet water temperature.

$$t_{w,out,pad} = \frac{-G_w \cdot c_{pw} \cdot t_{w,in,pad} + G_a \cdot c_{pea}\left[t_{wb,a,in,pad}\left(e^{\frac{(G_a c_{pea} - G_w c_{pw})k_s A_p}{G_a c_{pa} G_w c_{pw}}} - 1\right) + t_{w,in,pad}\right]}{G_a \cdot c_{pea} \cdot e^{\frac{(G_a c_{pea} - G_w c_{pw})k_s A_p}{G_a c_{pa} G_w c_{pw}}} - G_w \cdot c_{pw}} \tag{14}$$

To facilitate the calculation of analytical solutions, the number of transfer units of padding (NTU_2) and the heat capacity ratio can be defined in Eq. (15) and (16), and Eq. (14) can be simply expressed as Eq. (17). The analytical solutions of outlet air dry-bulb temperature and humidity can be solved by substituting Eq. (17) into Eq. (1) and (3). Where $t_{db,a,in,pad}$ and $\omega_{a,in,pad}$ are the inlet air dry-bulb temperature and humidity, and $\omega_{sat,a,in,pad}$ and $\omega_{w,in,pad}$ represent inlet air and water saturation humidity, respectively.

$$NTU_2 = \frac{k_s A_p}{G_a c_{pa}} \tag{15}$$

$$m = \frac{G_a c_{pea}}{G_w c_{pw}} \tag{16}$$

$$t_{w,out,pad} = \frac{m-1}{m \cdot e^{NTU_2(m-1)} - 1} t_{w,in,pad} + \frac{m\left(e^{NTU_2(m-1)} - 1\right)}{m \cdot e^{NTU_2(m-1)} - 1} t_{wb,a,in,pad} \tag{17}$$

$$t_{a,out,pad} = \left[\frac{e^{NTU_2(m-1)}\left(c_{pa} - m \cdot c_{pea}\right) + r_0 \cdot a}{c_{pa}\left(1 - m \cdot e^{NTU_2(m-1)}\right)} - e^{-NTU_2} - \frac{r_0 \cdot a}{c_{pa}}\right] t_{wb,a,in,pad} + \frac{e^{NTU_2(m-1)} - 1}{m \cdot e^{NTU_2(m-1)} - 1} t_{w,in,pad} + e^{-NTU_2} \cdot t_{db,a,in,pad} \tag{18}$$

$$\omega_{a,out,pad} = e^{-NTU_2} \cdot \omega_{a,in,pad} + \left(1 - e^{-NTU_2} - \frac{e^{NTU_2(m-1)} - 1}{m e^{NTU_2(m-1)} - 1}\right) \omega_{sat,a,in,pad} + \frac{e^{NTU_2(m-1)} - 1}{m e^{NTU_2(m-1)} - 1} \omega_{w,in,pad} \tag{19}$$

Similarly, the output air dry-bulb and water temperature of the sensible heat exchanger can be obtained in Eq. (22) and (23). Where k_L and A_{SHE} represent the heat transfer coefficient and area of the SHE, and $G_{a,SHE}$, and $G_{w,SHE}$ are the air and water mass flow rates of SHE. NTU_1 and n are the number of transfer units and heat capacity ratio of SHE, and $t_{w,in,SHE}$, $t_{w,out,SHE}$, $t_{a,in,SHE}$ and $t_{a,out,SHE}$ represent inlet and outlet temperature of water and air of SHE.

$$NTU_1 = \frac{k_L A_{SHE}}{G_{a,SHE} c_{pa}} \tag{20}$$

$$n = \frac{G_{a,SHE} c_{pa}}{G_{w,SHE} c_{pw}} \tag{21}$$

$$t_{w,out,SHE} = \frac{n-1}{n \cdot e^{NTU_1(n-1)} - 1} t_{w,in,SHE} + \frac{n\left(e^{NTU_1(n-1)} - 1\right)}{n \cdot e^{NTU_1(n-1)} - 1} t_{a,in,SHE} \tag{22}$$

$$t_{a,out,SHE} = \frac{e^{NTU_1(n-1)} - 1}{n \cdot e^{NTU_1(n-1)} - 1} t_{w,in,SHE} + \frac{n \cdot e^{NTU_1(n-1)} - e^{NTU_1(n-1)}}{n \cdot e^{NTU_1(n-1)} - 1} t_{a,in,SHE} \tag{23}$$

The experimental results obtained by previous reference [16] are used to verify the accuracy of analytical solutions, as shown in Fig. 4. The maximum absolute errors of padding and SHE output water temperature between theoretical and experimental results are 0.16 K and 0.26 K within the measuring error range of instrument, and relative errors are 0.99% and 1.23%. Experimental verification shows that the analytical solutions obtained by Eq. (17) ~ (19) and Eq. (22) ~ (23)

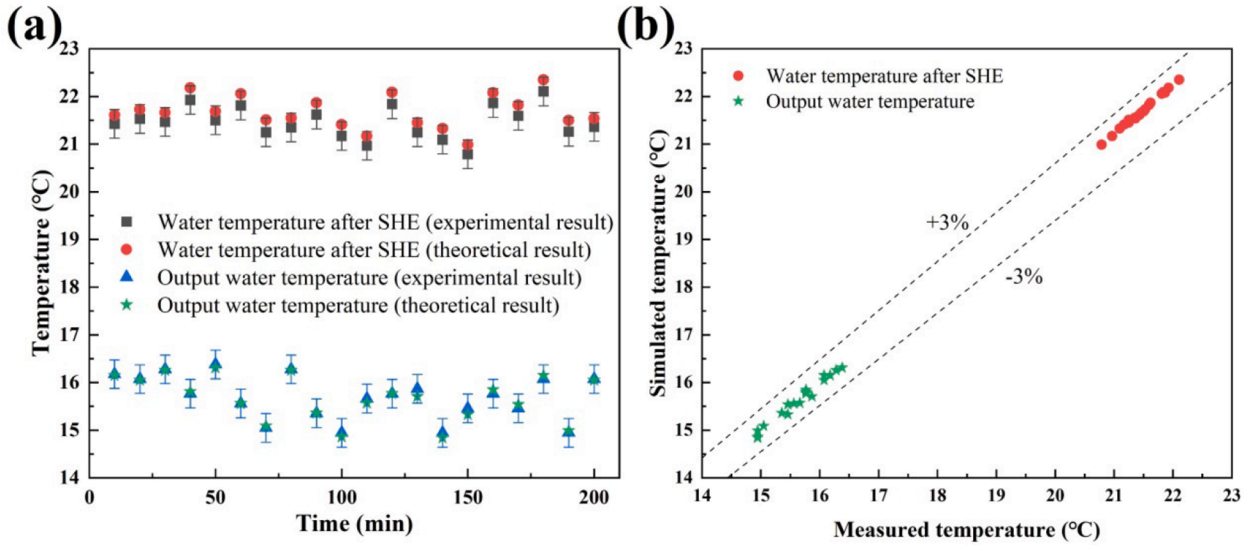

Fig. 4. The comparison of theoretical and experimental results. (a) Absolute error; (b) Relative error.

have high accuracy, and can be helpful for the application of water-mediated evaporative cooling. Theoretical solutions to counter-flow evaporative cooling can directly predict cooling performance of DEC and IEC based on design parameters and operating conditions.

3.3. Theoretical performance boundary

The analytical solution can be used not only to predict the output temperature but also to guide the selection of the water-mediated evaporative cooling process. This paper presents a method for comparing the performance of different water-mediated evaporative cooling processes without considering the initial investment and operational energy consumption in detail. When cooling capacity, NTU_2, air, and water mass flow rates are the same, it is considered that the evaporative cooling process with lower output temperature has better cooling performance. Taking the comparison of water-mediated direct evaporative cooling and series indirect evaporative cooling as an example, the known conditions satisfied by them are shown in Eq. (24) ~ (27).

$$Q_s = Q_{DEC} = G_{w,DEC}c_{pw}\left(t_{w,in,DEC} - t_{w,out,DEC}\right) = G_{w,s}c_{pw}\left(t_{w,in,s} - t_{w,out,s}\right) \quad (24)$$

$$G_{a,s} = G_{a,DEC} = G_a \quad (25)$$

$$G_{w,DEC} = G_{w,s,pad} = G_{w,s,SHE} = G_w \quad (26)$$

$$NTU_{2,DEC} = NTU_{2,s} = NTU_2 \quad (27)$$

Where Q_s and Q_{DEC} are the cooling capacities of series indirect and direct evaporative cooling, and $NTU_{2,s}$ and $NTU_{2,DEC}$ are the number of transfer units. $t_{w,in,DEC}$, $t_{w,out,DEC}$, $t_{w,in,s}$ and $t_{w,out,s}$ represent the inlet and output temperature of direct and series indirect evaporative cooling, and $G_{a,s}$, $G_{a,DEC}$, $G_{w,s}$ and $G_{w,DEC}$ represent air and water mass flow rates. Under the same conditions as above, indirect evaporative cooling needs to increase the initial investment of SHE, and energy consumption of fans and pumps is slightly higher than direct evaporative. This paper ignores the difference of initial investment and operating energy consumption and compares the cooling performance of different water-mediated evaporative cooling processes.

The evaporative cooling output water temperature varies continuously with outdoor meteorological conditions, and different evaporative cooling processes will have the same output temperature under some outdoor conditions. After sensible heat transfer of SHE, moisture and dew-point temperature of air remain unchanged, while air dry-bulb and wet-bulb temperatures decrease. Based on assumption 3, the wet-bulb temperature after SHE can be expressed as Eq. (28).

The meteorological parameter where the output water temperature of different water-mediated evaporative cooling processes is the same can be used as the performance boundary. Eq. (29) is the performance boundary between direct and series indirect evaporative cooling. Where $t_{a,in}$ and $t_{a,wb}$ are the inlet air dry-bulb and wet-bulb temperature and ΔT is the water temperature difference between inlet and outlet of evaporative cooling. The corresponding operating condition of this curve is that the inlet water temperature of series indirect evaporative cooling is equal to the inlet air dry-bulb temperature. The performance boundary is related to the difference between the dry-bulb temperature and the wet-bulb temperature of inlet air and can be reduced to Eq. (30) for m = 1.

$$\frac{t_{a,in,SHE} - t_{a,out,SHE}}{t_{a,in,SHE} - t_{dp,a,in,SHE}} = \frac{t_{wb,a,in,SHE} - t_{wb,a,out,SHE}}{t_{wb,a,in,SHE} - t_{dp,a,in,SHE}} \quad (28)$$

$$\frac{m\left(e^{NTU_2(m-1)} - 1\right)}{me^{NTU_2(m-1)} - 1}\left(t_{a,in} - t_{a,wb}\right) = \frac{Q}{G_w c_{pw}} = \Delta T \quad (29)$$

$$\frac{NTU_2}{NTU_2 + 1}\left(t_{a,in} - t_{a,wb}\right) = \frac{Q}{G_w c_{pw}} = \Delta T, \text{ while } m = 1 \quad (30)$$

In this paper, a validated model in the literature[16] is used to verify the accuracy of the performance boundary obtained from theoretical analysis, and lines 1 ~ 4 correspond to performance boundaries under different parameters as shown in Fig. 5. The relative error ranges of Line 1–4 in Fig. 5 are 1.58–7.87%, 0.22–2.89%, 4.39–14.36% and 1.58–4%, respectively. The errors between theoretical and simulated results are all smaller than 15%, which indicates that the analytical solutions Eq. (29) and (30) have high accuracy. The reason for the relatively large error of line 3 is that when ΔT is large, the air wet-bulb temperature in evaporative cooling also changes greatly. As can be seen in Fig. 3, when the air wet-bulb temperature changes greatly, the variation range of relative specific heat capacity sp_{ea} is also large, and assumption 3 is not valid.

When the humidity of inlet air is higher than that of the performance boundary, the output water temperature of direct evaporative cooling is lower than series indirect evaporative cooling. On the contrary, the output water temperature of series indirect evaporative cooling is lower than that of direct evaporative cooling when outdoor air is dry and hot. Therefore, the performance boundary can be applied to divide the psychrometric chart into two regions, with the wet side having a better cooling performance by direct evaporative cooling and the dry region

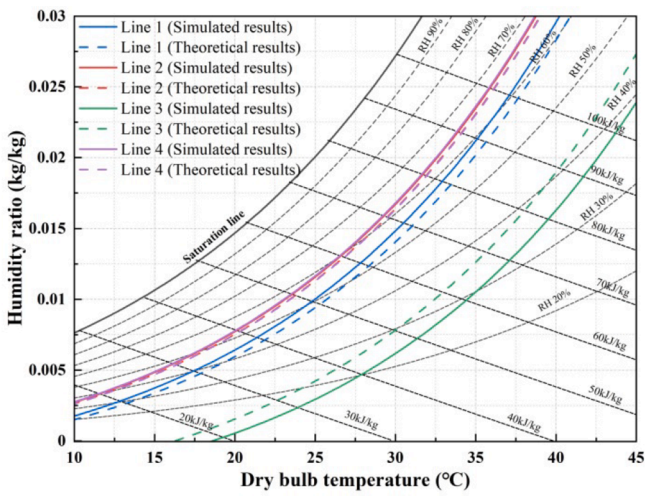

Fig. 5. Theoretical and simulated results comparing the performance of DEC and series IEC.Line 1: $m = 1$, $NTU_1 = 2$, $NTU_2 = 2$, $\Delta T = 5$ K; Line 2: $m = 1.5$, $NTU_1 = 2$, $NTU_2 = 2$, $\Delta T = 5$ K; Line 3: $m = 1$, $NTU_1 = 2$, $NTU_2 = 2$, $\Delta T = 9$ K; Line 4: $m = 1$, $NTU_1 = 2$, $NTU_2 = 5$, $\Delta T = 5$ K.

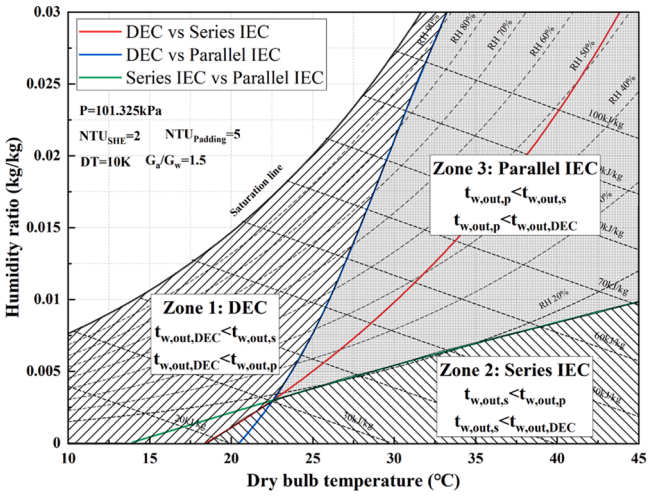

Fig. 6. Performance partitions of evaporative cooling processes.($NTU_{SHE} = 2$, $NTU_{padding} = 2$, $\Delta T = 5$ K, $G_a/G_w = 1$).

having a better performance by series indirect evaporative cooling.

This performance boundary can be used to select the appropriate evaporative cooling process when the design parameters are determined, or to select appropriate design parameters when the evaporative cooling process is determined. Design parameters mainly include air mass flowrate, water mass flowrate, cooling capacity, NTU_1 and NTU_2. Water-mediated evaporative cooling processes mainly include series indirect evaporative cooling, parallel indirect evaporative cooling, and direct evaporative cooling. Concise analytical solutions of the performance boundary between DEC and parallel IEC and between parallel IEC and series IEC cannot be obtained by theoretical analysis.

4. Performance comparison

Common water-mediated evaporative cooling processes are direct evaporative cooling, series indirect evaporative cooling, and parallel indirect evaporative cooling. In the previous section, the performance boundary between DEC and series IEC has been obtained theoretically, and the psychrometric chart can be divided into two applicable regions for DEC and series IEC. Performance boundaries between DEC and parallel IEC and between series IEC and parallel IEC will be obtained using a validated model[16] in this section. In the simulation of this section, the SHE of parallel IEC always satisfies the equal heat capacity of air and water, and its value is about one-fourth of the water heat capacity of evaporation according to Fig. 3. Three water-mediated evaporative cooling processes are compared under the same cooling capacity.

4.1. Performance partitions of evaporative cooling processes

Simulation results of the performance boundary are shown in Fig. 6, which are the performance boundaries between DEC and series IEC, DEC and parallel IEC, and series IEC and parallel IEC, respectively. When the inlet air humidity is greater than the performance boundary between DEC and series IEC, the output water temperature of DEC is lower than that of series IEC. When the inlet air humidity is greater than the performance boundary between DEC and parallel IEC, the output water temperature of DEC is lower than that of parallel IEC. Similarly, when the inlet air humidity is greater than the performance boundary between series IEC and parallel IEC, the output water temperature of parallel IEC is lower than that of series IEC.

Three simulated performance boundaries divide the psychrometric chart into three regions. When the outdoor meteorological parameter is located in a certain zone, the output water temperature of the evaporative cooling process corresponding to that zone is the lowest. For example, if the state point of outdoor air is in zone 1, the output water temperature of DEC is the lowest under this condition. It is possible to determine which kind of evaporative cooling process is applicable in different regions according to the climate range on the psychrometric chart.

The performance comparison of evaporative cooling processes has two uses: one is to select the appropriate process under determining design parameters; the second is to optimize the design parameters under the defined evaporative cooling process. When design parameters of evaporative cooling are known, the appropriate process can be selected to refer to the proportion of meteorological points falling on different zones of the psychrometric chart. Engineers can also improve evaporative cooling performance by optimizing design parameters to expand the climate applicability of the selected process. Therefore, the variation of performance partitions under different design parameters is very important for the application of evaporative cooling processes.

4.2. Influence of heat and mass transfer coefficient

The heat and mass transfer coefficient of the padding has the greatest impact on performance, and also affects the performance partition of different evaporative cooling processes. Fig. 7(a)~(e) shows the performance partitions under different $NTU_{padding}$, and constant conditions are that $NTU_{SHE} = 2$, $\Delta T = 5$ K and $G_a/G_w = 1$. Fig. 7(f) is the output water temperature of different water-mediated evaporative cooling versus $NTU_{padding}$ when the outdoor dry-bulb temperature is 35℃ and the relative humidity is 60%.

Under this setting and common conditions of evaporative cooling processes, the applicable ranges of DEC and series IEC occupy almost the entire psychrometric chart, and parallel IEC has little prospect of being used. With the improvement of the heat and mass transfer coefficient of the padding, the applicable climate range of parallel IEC is significantly increased, while the applicable range of DEC is reduced. The series IEC should be applied in dry regions, and the DEC is mainly used in wet regions. It is only possible to apply parallel IEC in some hot and humid regions if the padding performance is excellent.

Under the same meteorological condition as Fig. 7(f), with the increase of $NTU_{padding}$, the output water temperature of three water-mediated evaporative cooling processes decreases. In the $NTU_{padding}$ range of 1.66 ~ 3.26, the series IEC has the best performance, DEC has the best performance when $NTU_{padding}$ is lower than 1.66, and parallel

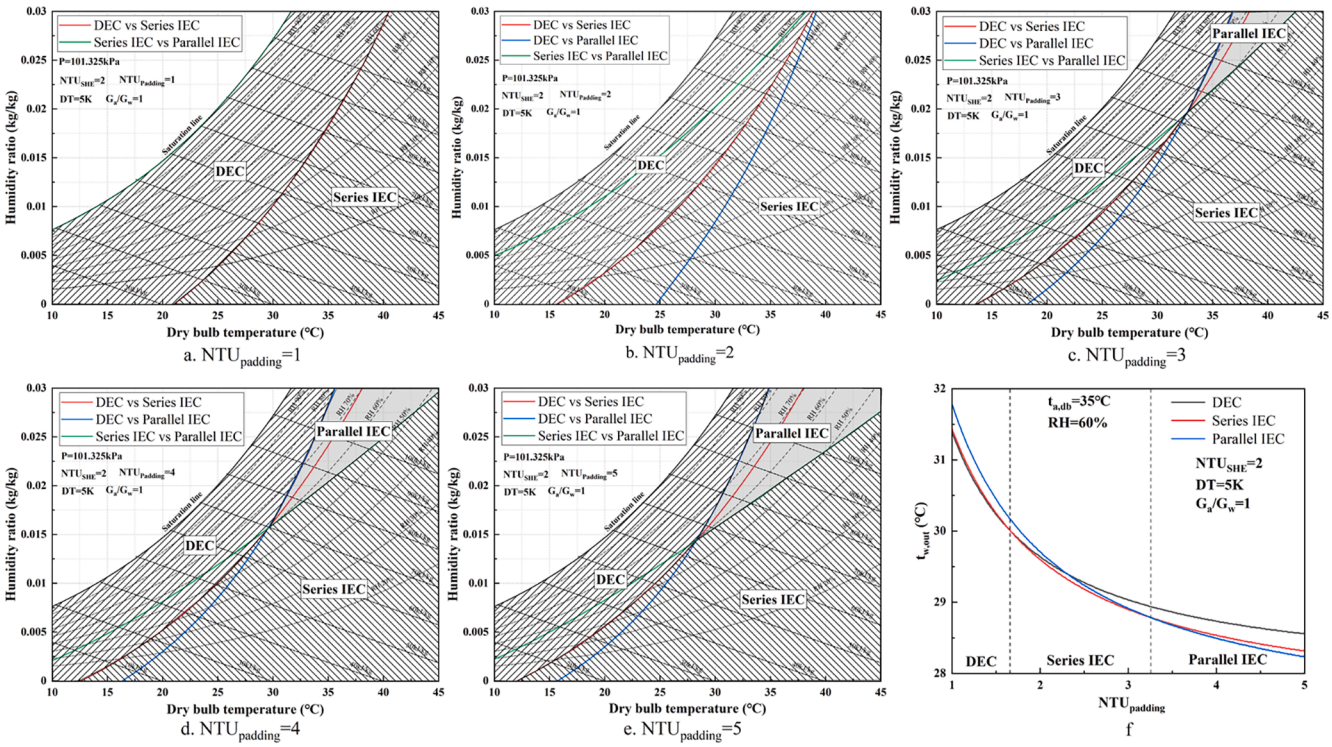

Fig. 7. Performance comparison of evaporative cooling processes under different $NTU_{padding}$. (NTU_{SHE} = 2, ΔT = 5 K, G_a/G_w = 1).

IEC produces the coldest water when $NTU_{padding}$ is higher than 3.26.

To increase the evaporative cooling performance, one of the main optimized directions is to improve the padding performance, such as wettability, ripple pattern, and channel aspect ratio. When the heat and mass transfer performance per unit volume of padding is fixed, $NTU_{padding}$ can be increased by increasing the padding volume, such as increasing the height or the upwind area. With the increases in padding height, the wind resistance and power consumption of fans will increase, and it also leads to the poor effect of the water distribution at the bottom of the padding. Increasing the upwind area may also lead to problems with water distribution and wetting rate due to reducing water mass flow rate per unit upwind area.

It also indicates that increasing the padding heat and mass transfer coefficient is more beneficial for IEC. Indirect evaporative cooling uses

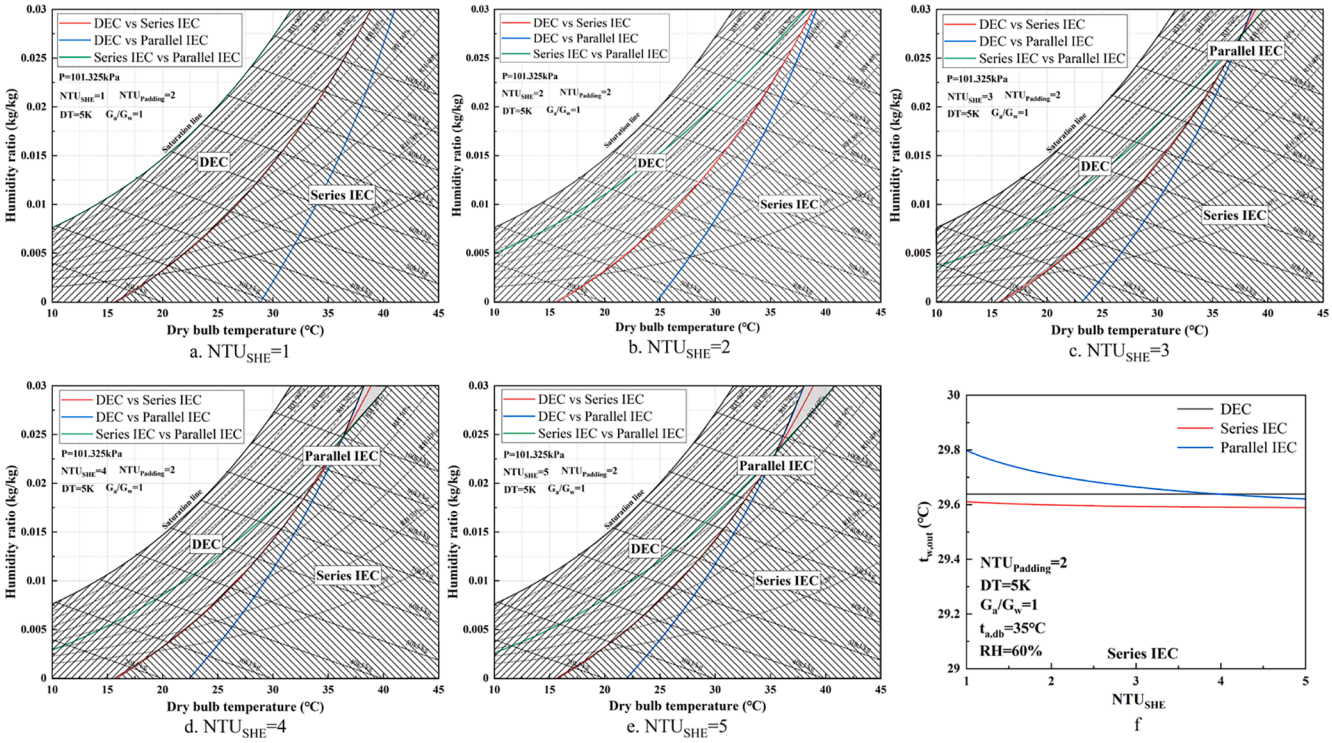

Fig. 8. Performance comparison of evaporative cooling processes under different NTU_{SHE}.($NTU_{padding}$ = 2, ΔT = 5 K, G_a/G_w = 1).

sensible heat exchangers to pre-cool outdoor air to obtain lower temperature-producing water. Under the same cooling capacity, the heat exchange in the padding of IEC is greater than that of DEC, so IEC is more eager for high-performance padding. Series IEC uses inlet water to pre-cool outdoor air, while parallel IEC uses part of producing water to cool air. In most cases, the heat transfer of parallel IEC is greater than that of both DEC and series IEC, which requires the highest heat and mass transfer performance. In summary, DEC is preferred for low padding performance, series IEC should be used more for medium performance, and parallel IEC should be considered for excellent padding performance.

The heat transfer coefficient of sensible heat exchangers affects the pre-cooling process of air, while direct evaporative cooling does not have this process and equipment. Fig. 8 indicates the influence of NTU_{SHE} on different performance partitions and output water temperatures of evaporative cooling processes. According to Eq. (29) and Fig. 8 (a)~(e), the performance dividing line between DEC and series IEC is independent of NTU_{SHE}. The heat transfer coefficient of SHE indirectly influents the output water temperature of evaporative cooling by affecting the pre-cooling process. The heat transfer coefficient of SHE has little influence on the selection of the evaporative cooling process and output water temperature, and performance partitions almost do not change accordingly.

The sensible heat exchanger is a water–air non-contact heat transfer device composed of metal tubes and fins, the initial investment of which is significantly higher than that of padding under the same NTU. Therefore, when indirect evaporative cooling is selected, more volumes of high-quality padding and suitable scale sensible heat exchangers should be set. The appropriate NTU of SHE should be around 2 according to Fig. 8(f), and the selection of NTU should also consider anti-freezing performance requirements for some application scenarios.

4.3. Influence of the air–water ratio

Water-mediated evaporative cooling takes cooling water as the final product, and the air–water ratio is an important parameter affecting output temperature. Fig. 3 shows that the equivalent specific heat capacity of air is close to that of water in the process of evaporative cooling, which indicates that the reasonable range of air–water ratio should be around 1. Fig. 9 shows the performance partitions and output temperatures for different evaporative cooling processes at the air–-water ratio of 0.5 to 2.

With the increase in the air–water ratio, the performance partition of DEC decreases, while the applicable range of parallel IEC increases. Under the same meteorological condition as Fig. 9(e), the output water temperature decreases with the increase in air–water ratio. At a larger air–water ratio, the water cooled by evaporation can more easily approach the inlet air wet-bulb temperature, and the outlet water temperature of SHE is also close to the inlet air dry-bulb temperature.

The heat transfer of IEC is significantly greater than DEC due to the presence of a pre-cooling process at the same cooling capacity. And the heat exchange of parallel IEC, which uses product water for pre-cooling, is higher than that of series IEC. Therefore, the order of the total heat transfer from the largest to the smallest is generally parallel IEC, series IEC, and DEC. The larger the air mass flow rate, the more conducive to the transfer of heat and mass, which leads to the change in the climate application range of different evaporative cooling processes under different air–water ratios.

No matter which water-mediated evaporative cooling process is applied, the increasing air–water ratio of the padding is an important way to optimize the cooling performance, mainly by increasing the frontal airspeed. The larger frontal airspeed, on the one hand, leads to greater wind resistance, on the other hand, promotes the water droplets carrying phenomenon and reduce the wetting rate. The increase in the air–water ratio will increase the power consumption and water consumption of evaporative cooling, and more attention should be paid to the adverse effect on the wetting rate and the reduction of padding heat and mass transfer performance.

4.4. Influence of inlet and outlet water temperature difference

In the case of the same water mass flow rate, the temperature

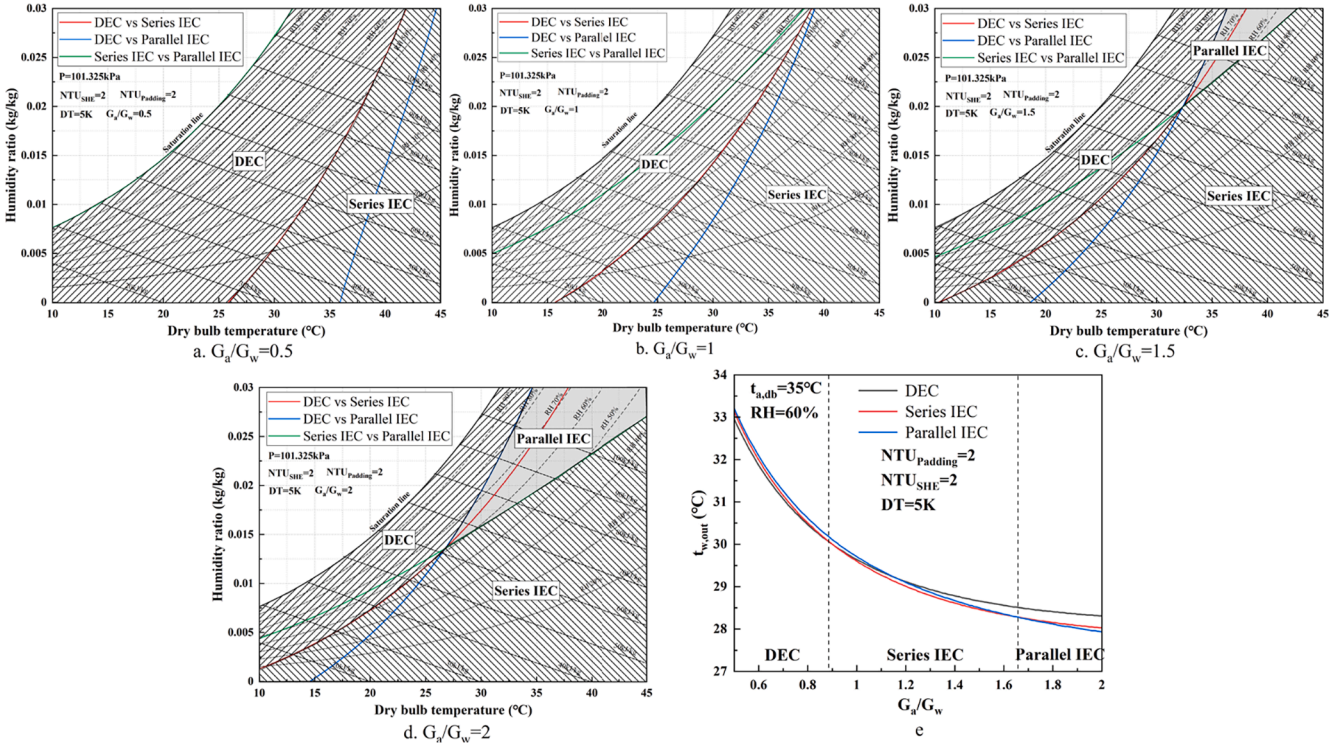

Fig. 9. Performance partitions and output temperatures versus air–water ratios.($NTU_{SHE} = 2$, $NTU_{padding} = 2$, $\Delta T = 5$ K).

difference between inlet and outlet water determines the evaporative cooling capacity. To meet the cooling needs of different types of buildings due to different objects, the designed temperature difference of evaporative cooling is also different. For example, when the service object is personal, the air conditioner deals with returned air to the product air is usually a small temperature difference. When air conditioning equipment is used to cool fresh air, it is often a large temperature difference process to cool fresh air from outdoor dry-bulb temperature to product air temperature. As the cooling system serves some devices, such as chips and power transformers, the operating temperature is relatively higher than humans, and the temperature difference is also greater than the common system. Therefore, for common residential and commercial buildings, the temperature difference between inlet and outlet water of evaporative cooling is usually small, while cooling for data center and power equipment, evaporative cooling should be designed with a large temperature difference.

Fig. 10 indicates the variation of performance partitions and output temperatures of three water-mediated evaporative cooling processes under different temperature differences. Under the current design conditions of $NTU_{SHE} = 2$, $NTU_{padding} = 2$, and $G_a/G_w = 1$, the larger temperature difference facilitates the application of DEC, which gradually expands the performance partition until it occupies almost the entire psychrometric chart. The increase in temperature difference means that the cooling capacity per unit water mass flow rate increases, so that the output and inlet water temperature will also increase as in Fig. 10(f).

When the temperature difference and the cooling capacity increase, the inlet water temperature of series IEC may exceed the outdoor air dry-bulb temperature, and SHE loses the function of pre-cooling, the performance of which deteriorates sharply. More cooling capacity leads to greater heat exchange of IEC padding, and DEC performs better than IEC when the heat transfer coefficient and air–water ratio are small.

4.5. Performance partitions in the ideal case

The previous sections simulated the effects of design parameters on the performance partitions and output temperatures of different water-mediated evaporative cooling processes. To improve evaporative cooling performance in the future, increasing the padding transfer units and the air–water ratio is the common development direction. Increasing the heat transfer coefficient and area of SHE cannot significantly improve the IEC cooling performance and the initial investment is high, so NTU_{SHE} can be maintained in the appropriate range. The temperature difference between inlet and output water is determined by user and system form. Therefore, the ideal equipment is with excellent padding performance and a large air–water ratio, and engineers in these conditions select the appropriate water-mediated evaporative cooling process according to the cooling system's designed requirements.

Fig. 11 shows the variations of performance partitions and output temperatures in the ideal case under different temperature differences. When the temperature difference between supplied and returned water is small, the area of the application zone of the three evaporative cooling technologies is similar. As the temperature difference increases, the application range of DEC and parallel IEC increases, while that of series IEC decreases. Fig. 11 represents the applicable zone of various water-mediated evaporative cooling processes under ideal conditions, and almost the maximum applicable zone of IEC.

5. Selection of evaporative cooling process

It is a difficult problem for evaporative cooling technology to select the appropriate process in different systems with various cooling requirements. For a single designed meteorological parameter point or meteorological parameter points that are concentrated in a certain performance partition, the appropriate process can be easily chosen by applying the above performance partitions on the psychrometric chart under a different system designed parameters. When meteorological parameters of the cooling season are distributed in different performance zones, how do select the appropriate evaporative cooling process?

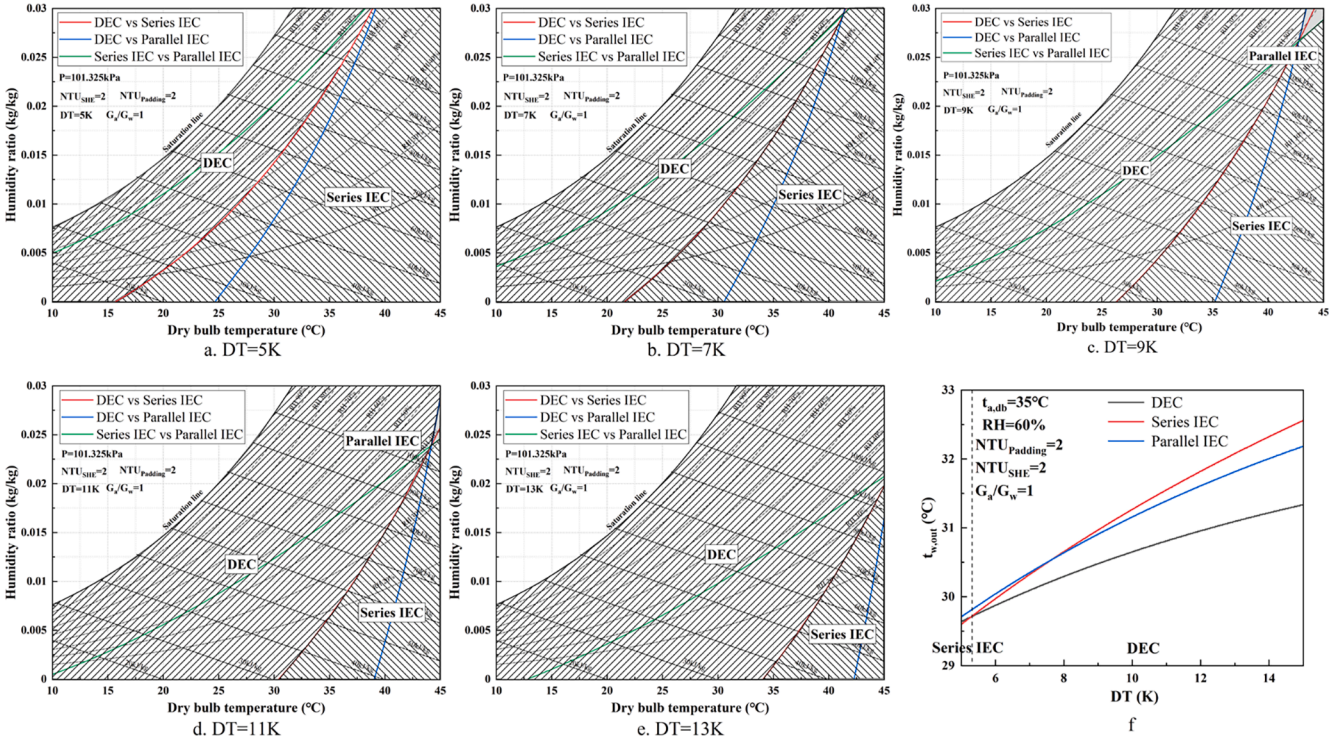

Fig. 10. Performance partitions and output temperatures versus water temperature differences.($NTU_{SHE} = 2$, $NTU_{padding} = 2$, $G_a/G_w = 1$).

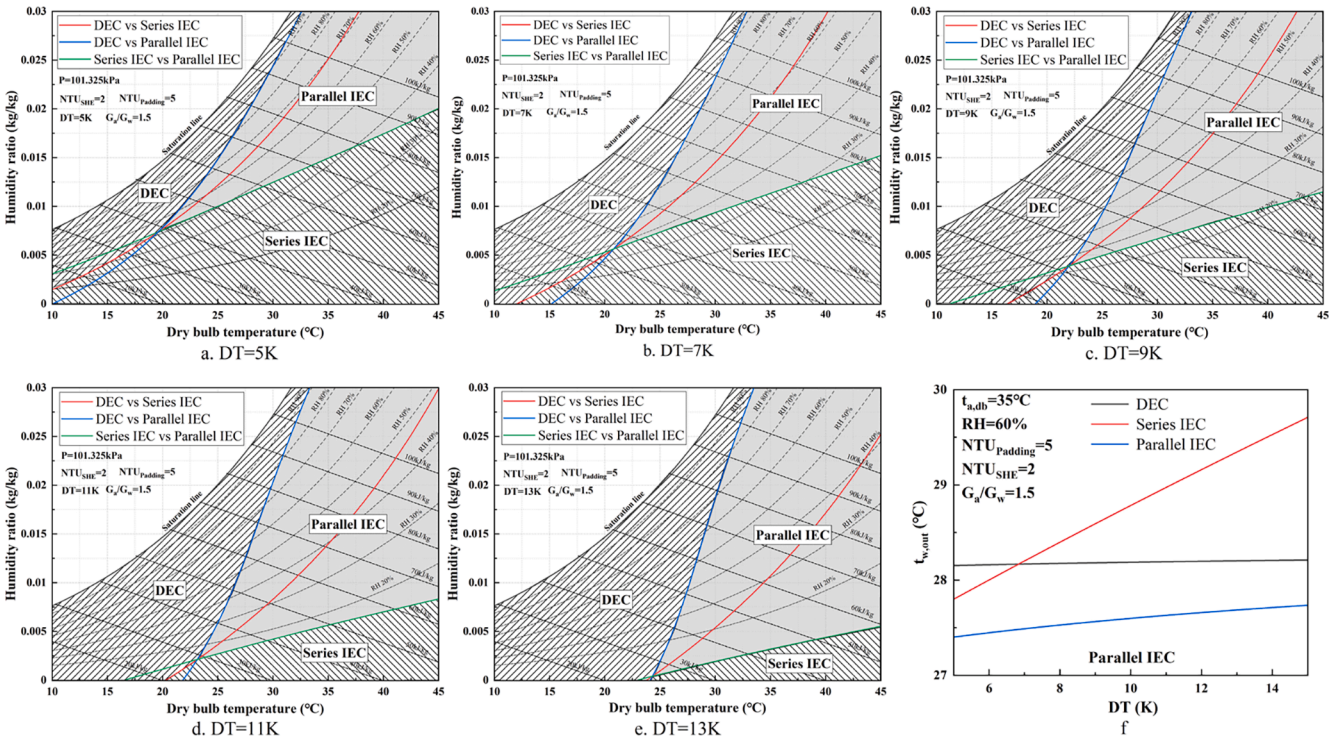

Fig. 11. Performance partitions and output temperatures versus water temperature differences in the ideal case. ($NTU_{SHE} = 2$, $NTU_{padding} = 5$, $G_a/G_w = 1.5$).

5.1. Method and limitation

The common approach is to model all evaporative cooling processes, simulate their performance, and select the appropriate process, but it requires extreme expertise in evaporative cooling simulation and is not suitable for large-scale applications. A simple method to think about is proposed to select the appropriate process by using partitions of different evaporative cooling technologies in the psychrometric chart.

The selection of the evaporative cooling process is influenced by three factors: cooling system requirements, local meteorological conditions and evaporative cooling designed parameters. The anti-freezing requirements should be properly considered when selecting an evaporative cooling process, and series IEC and parallel IEC can significantly reduce the labor cost, power consumption, and water consumption of deicing. The previous sections have analyzed the performance partitions of water-mediated evaporative cooling processes on the psychrometric chart for different designed parameters.

First and foremost, the set of all outdoor meteorological parameter points needs to be collected by considering the requirements of the actual cooling system, eliminating parameter points that are not in operation and have little impact on performance. Engineers can determine which evaporative cooling performs better based on the proportion of meteorological parameters that fall into different performance partitions. When the proportion of outdoor meteorological parameter points falling on the performance zone of one evaporative cooling process is significantly higher than that of the other, it indicates that the performance of this evaporative cooling process dominates for a longer time. This method can be divided into the following four steps.

Step 1: Select the corresponding performance partition diagram according to the evaporative cooling designed parameters.

Step 2: Collect all the meteorological parameter points when evaporative cooling equipment operates.

Step 3: Calculate the proportion of meteorological parameter points falling in different performance partitions.

Step 4: Select the appropriate process according to the proportions of different evaporative coolers.

This method can be used as a reference for selection in most cases, but it does not show that the performance of the evaporative cooling process with a larger proportion is always better, especially when the proportion difference is small. When the proportions of different evaporative cooling processes are close, IEC generally outperforms DEC, and parallel IEC generally outperforms series IEC. The proportion only reflects the length of time that each evaporative cooling process is at its optimal performance, not reflects how much lower the output water temperature of this process is than that of the other process.

5.2. Case study

A case cooling system will be presented to illustrate the applicability and limitation of different water-mediated evaporative cooling processes in 16 cities around the world. Considering the future development of padding properties, the designed parameters of evaporative cooling in this paper are all under ideal conditions. The number of transfer units of padding is 5, the number of transfer units of SHE is 2, and the air–water ratio is 1.5. The meteorological data of these cities in 2020 are adopted as the basis for the selection of the evaporative cooling process. Three water-mediated evaporative cooling processes are compared under the same cooling capacity.

This case presents a cooling system using evaporative cooling as the independent cold source to provide cooling capacity directly to users. The cooling water circulates between users and evaporative cooling, the temperature difference of which is 5 K. It is assumed that the business hours are 10:00 ~ 22:00 and the cooling system is turned on when the outdoor dry-bulb temperature exceeds 20℃, and there is no anti-freezing requirement. Lower output water temperature of evaporative cooling indicates better performance, so a performance partition diagram can still guide engineers select the appropriate process. The meteorological parameters that meet the requirement and are during business hours of Beijing, Tehran, and Paris are represented in the corresponding performance partition diagram, as shown in Fig. 12.

According to the distribution of meteorological parameters on the psychrometric chart of different cities, the proportion falling in different

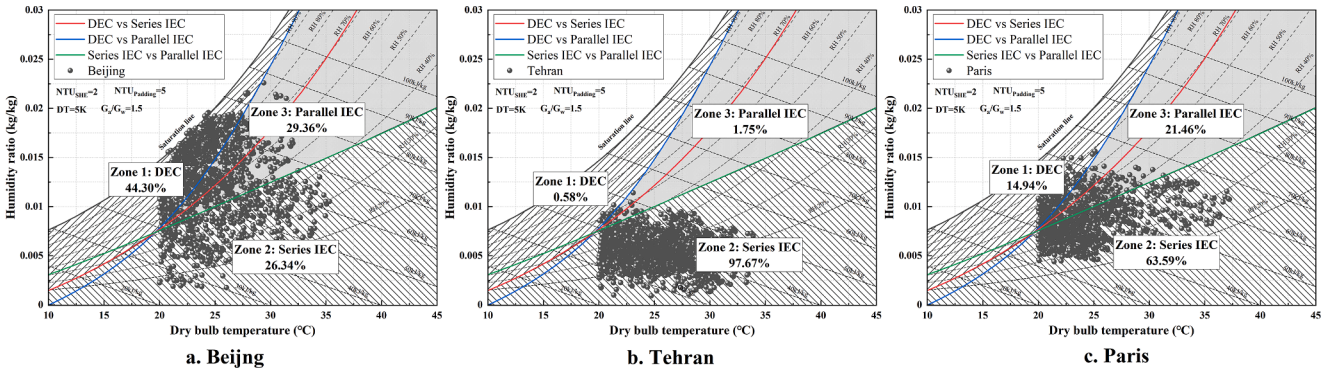

Fig. 12. The distribution of meteorological parameters for Beijing, Tehran, and Paris on the psychrometric chart. ($NTU_{SHE} = 2$, $NTU_{padding} = 5$, $G_a/G_w = 1.5$, $\Delta T = 5$ K).

performance zones can be calculated. The meteorological parameters in Beijing are distributed in three zones, and the proportions in DEC, series IEC, and parallel IEC zones are 44.30%, 26.34%, and 29.36%, respectively. Similarly, Tehran has proportions of 0.58%, 97.67%, and 1.75%, and Paris has proportions of 14.94%, 63.59%, and 21.46%, and proportions of other cities can also be calculated as shown in Fig. 13. Whether the evaporative cooling process with the largest proportion of meteorological parameters should be selected? Output water temperatures of three evaporative cooling processes are simulated and also represented in Fig. 13, and the average output water temperature is calculated by the following formula where H is time.

$$\bar{t}_{w,out} = \frac{\int t_{w,out} dH}{H} \tag{31}$$

Cities with the largest proportion of meteorological parameters falling into the DEC performance zone generally have higher output water temperature and may require vapor compression chillers to replenish cooling capacities, such as Beijing, Canberra, Guangzhou, Harbin, and Kunming. Cities with the largest proportion falling in series IEC zone generally have lower output water temperature, such as Ankara, Berlin, Brussels, London, Madrid, Moscow, Paris, San Francisco, Tehran, and Urumqi. The process with the highest proportion and with the lowest average output water temperature in different cities is shown in Table 1 according to Fig. 13.

Table 1
The process with the largest proportion and with the lowest average output temperature in different cities.

City	The process with the largest proportion	The process with the lowest average output temperature
Ankara	Series IEC	Series IEC
Beijing	DEC	Parallel IEC
Berlin	Series IEC	Series IEC
Brussels	Series IEC	Series IEC
Canberra	DEC	Parallel IEC
Guangzhou	DEC	DEC
Harbin	DEC	Parallel IEC
Kunming	DEC	DEC
London	Series IEC	Series IEC
Madrid	Series IEC	Series IEC
Moscow	Series IEC	Series IEC
New York	Parallel IEC	Parallel IEC
Paris	Series IEC	Series IEC
San Francisco	Series IEC	Series IEC
Tehran	Series IEC	Series IEC
Urumqi	Series IEC	Series IEC

Under the premise of this case, the average output water temperature of the evaporative cooling process with the largest proportion of most cities is also the lowest. Series IEC has the best performance in most

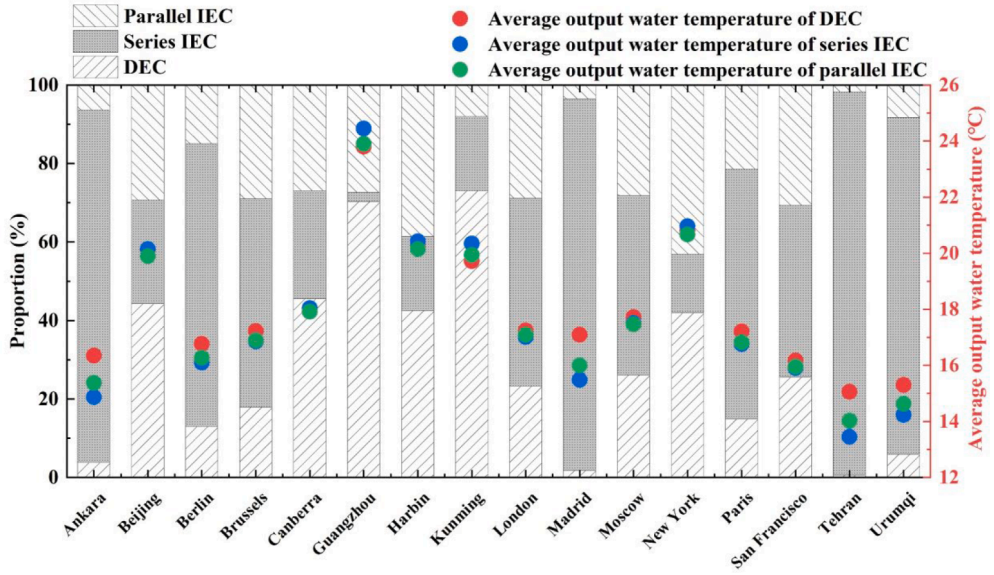

Fig. 13. Proportions of meteorological parameters and simulated average output water temperature of different evaporative cooling processes in different cities. ($NTU_{SHE} = 2$, $NTU_{padding} = 5$, $G_a/G_w = 1.5$, $\Delta T = 5$ K).

cities and parallel IEC is selected in a few cities, and even DEC is suitable for fewer cities. This shows that it is feasible to select the appropriate process according to proportions of meteorological parameters falling in different performance zones with an accuracy of 81.25%, especially when selecting series IEC and parallel IEC such as Ankara, Berlin, Brussels, London, Madrid, Moscow, New York, Paris, San Francisco, Tehran, and Urumqi. But the average output water temperature of the evaporative cooling process with the largest proportion in Beijing, Canberra, and Harbin is even higher than other processes, which suggests that this method of selecting process based on proportions does not work in these cities. Fig. 14 can explain why some cities have the highest proportion in the DEC zone, but the optimal process is not DEC.

Fig. 14 shows the output water temperature and temperature difference of different evaporative cooling processes under various meteorological parameters. Fig. 14(a) is the minimum output water temperature of three processes, which is the output water temperature of the process in each performance zone. Isotherms in the DEC performance zone coincide with the *iso*-wet-bulb temperature line, and isotherms of series IEC and parallel IEC zones are between the *iso*-wet-bulb and the *iso*-dew-point temperature line, and series IEC is closer to the so-dew-point temperature line compared with parallel IEC.

Fig. 14(b), (c) and (d) show the output temperature differences between DEC and series IEC, DEC and parallel IEC, and series IEC and parallel IEC, respectively. The temperature differences between DEC and series IEC and DEC and parallel IEC are larger than that between series IEC and parallel IEC. However, the DEC performance zone is relatively narrow, and DEC output water temperature under meteorological conditions falling in DEC performance is at most 1.87 K lower than the output temperature of other processes, while output temperature in series and parallel IEC performance zones can be 6.41 K lower than DEC. This is the reason why some cities have the largest proportion of meteorological parameters falling into the DEC performance zone, but DEC is not the most appropriate process. For Beijing, Canberra, and Harbin, the proportion of DEC is about 50% and the most suitable process for these cities is parallel IEC. For Guangzhou and Kunming, where the proportion of DEC zone exceeds 70%, DEC is still the best performing process.

This case study analyzes the selection of evaporative cooling processes for a particular cooling system in 16 global cities and illustrates the effectiveness of this method of selecting processes according to the proportions of meteorological parameter points falling in performance partitions. When the proportion of series or parallel IEC is maximum, it is the most appropriate process, while when the proportion of DEC is the largest, other methods should be used to further determine whether DEC is still selected.

The selected process is different under various designed cooling system parameters, series IEC is more widely applied in this case. According to the performance comparison study in section 4, the range of DEC application increases with the decrease in air–water ratio and $NTU_{padding}$. To adapt to the future development direction of evaporative cooling, the temperature difference between returned and supplied water will be further increased. In this situation, DEC and parallel IEC

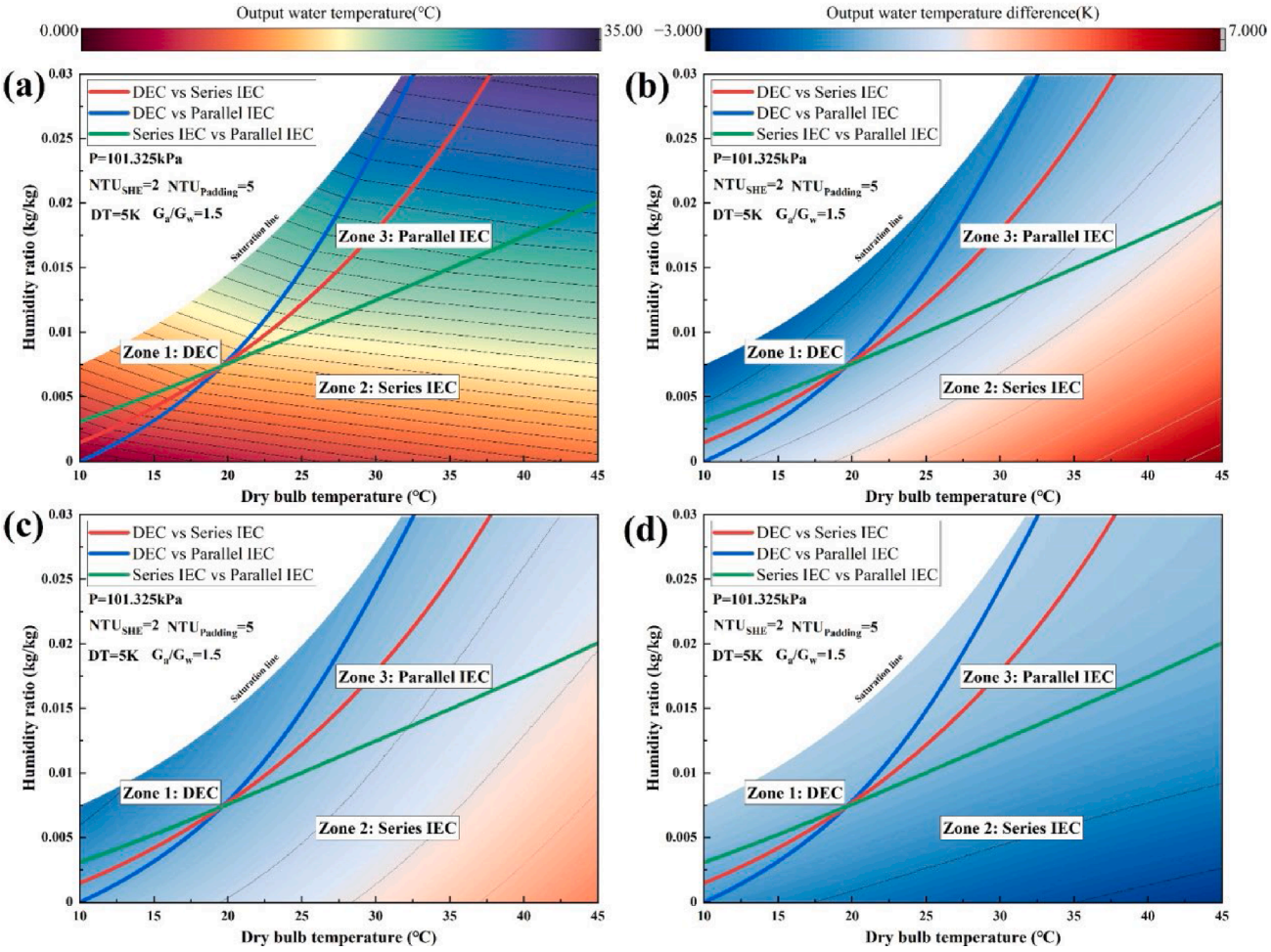

Fig. 14. Output water temperature and temperature difference of DEC, series IEC, and parallel IEC. ($NTU_{SHE} = 2$, $NTU_{padding} = 5$, $G_a/G_w = 1.5$, $\Delta T = 5$ K) (a) the lowest output water temperature within each performance partition; (b) output water temperature difference of DEC and series IEC; (c) output water temperature difference of DEC and parallel IEC; (d) output water temperature difference of series IEC and parallel IEC.

will be valued, while series IEC is not suitable for these scenarios such as cooling for data centers, power transformers, and fresh air.

6. Conclusions

This paper presents a theoretical study for comparing three water-mediated evaporative cooling technologies: DEC, series IEC and parallel IEC. By comparing the performance of various evaporative coolers under different system design parameters and climatic conditions, the following conclusions can be drawn:

(1) Simple theoretical solutions of counter-flow evaporative cooling are given to reduce computational efforts. The maximum absolute and relative errors of the solutions are 0.26 K and 1.23%. The heat transfer coefficient of the combined heat and mass transfer is cp_{ea}/cp_a (2.72–4.95) time than the pure heat transfer process if there were no mass transfer.
(2) The climatic dividing line between DEC and series IEC is derived, which is related to the difference between outdoor dry-bulb and wet-bulb temperature. This also shows that there are clear climatic dividing lines between different evaporative cooling technologies only related to design parameters.
(3) Performance partitions on the psychrometric chart of three water-mediated evaporative cooling are given with various design parameters. DEC works best in a temperate and humid climate, while series IEC is more efficient in a dry climate, and parallel IEC is the best choice for hot and semi-humid climates. The increase in SHE and padding heat transfer coefficients and air–water flowrate ratio will expand the range in the psychometric chart where IECs work the best, and a greater temperature difference will broaden DEC and parallel IEC performance partitions.
(4) A simpler method for selecting the appropriate evaporative cooling technology is proposed based on the proportions of climate parameters falling into different performance partitions outlined above. This method is verified by a case study of 16 global cities with a relative error of 19.75%, which is accurate and feasible, particularly when selecting series IEC and parallel IEC. This method cannot accurately distinguish DEC and IEC, because the proportion of climatic parameters only reflects the duration performing best of each evaporative cooling, and it still needs to use mathematical simulation to deeply compare the annual performance.

While the paper focuses on comparative studies of three water-mediated evaporative cooling technologies in order to guide the selection of appropriate processes in different scenarios, techno-economic analysis and experimental studies of the technologies investigated should be carried out to comprehensively display the potential and benefits of evaporative cooling in terms of application in different regions as replacement or pre-cooling of mechanical vapor compression chillers.

CRediT authorship contribution statement

Yang Jing: Conceptualization, Methodology, Software, Validation, Formal analysis, Investigation, Data curation, Resources, Writing – original draft, Writing – review & editing, Visualization. **Xiaoyun Xie:** Writing – original draft, Writing – review & editing, Supervision, Project administration, Funding acquisition. **Yi Jiang:** Supervision, Project administration, Funding acquisition.

Declaration of Competing Interest

The authors declare that they have no known competing financial interests or personal relationships that could have appeared to influence the work reported in this paper.

Data availability

Data will be made available on request.

Acknowledgment

The authors gratefully acknowledge the support from National key research and development program of China (key projects of international cooperation in science and technology innovation) (Grant number 2019YFE0102700).

References

[1] IEA, World Energy Outlook 2021. 2021, IEA. p. 383.
[2] Yang L, Yan H, Lam JC. Thermal comfort and building energy consumption implications – A review. Appl Energy 2014;115:164–73.
[3] Pérez-Lombard L, Ortiz J, Pout C. A review on buildings energy consumption information. Energ Buildings 2008;40(3):394–8.
[4] Rong H, et al. Optimizing energy consumption for data centers. Renew Sustain Energy Rev 2016;58:674–91.
[5] 2020 ASHRAE Handbook - HVAC Systems and Equipment (SI Edition). 2020: American Society of Heating Refrigerating and Air-Conditioning Engineers Inc. ASHRAE.
[6] Delfani S, et al. Energy saving potential of an indirect evaporative cooler as a pre-cooling unit for mechanical cooling systems in Iran. Energ Buildings 2010;42(11):2169–76.
[7] Porumb B, Bălan M, Porumb R. Potential of Indirect Evaporative Cooling to Reduce the Energy Consumption in Fresh Air Conditioning Applications. Energy Procedia 2016;85:433–41.
[8] Yang Y, Cui G, Lan CQ. Developments in evaporative cooling and enhanced evaporative cooling - A review. Renew Sustain Energy Rev 2019;113:109230.
[9] Lin C, et al. Design and application of evaporative cooler for a freezer. Appl Therm Eng 2020;178:115411.
[10] Zheng B, et al. An analytical model for cross-flow indirect evaporative cooling considering condensation under various fresh air conditions. Energy Procedia 2019;158:5747–52.
[11] Jafarian H, Sayyaadi H, Torabi F. Modeling and optimization of dew-point evaporative coolers based on a developed GMDH-type neural network. Energ Conver Manage 2017;143:49–65.
[12] Anisimov S, Pandelidis D. Numerical study of the Maisotsenko cycle heat and mass exchanger. Int J Heat Mass Transf 2014;75:75–96.
[13] Mahdi AH, Ali Aljubury IM. Experimental investigation of two-stage evaporative cooler powered by photovoltaic panels using underground water. Journal of Building. Engineering 2021;44:102679.
[14] Sohani A, Sayyaadi H, Azimi M. Employing static and dynamic optimization approaches on a desiccant-enhanced indirect evaporative cooling system. Energ Conver Manage 2019;199:112017.
[15] Costelloe B, Finn D. Indirect evaporative cooling potential in air – water systems in temperate climates. Energ Buildings 2003.
[16] Jing Y, et al. Optimization and performance analysis of water-mediated series indirect evaporative chillers: Experimental and simulated investigation. Energ Conver Manage 2022;268:115990.
[17] Jiang Y, Xie X. Theoretical and testing performance of an innovative indirect evaporative chiller. Sol Energy 2010;84(12):2041–55.
[18] Jain JK, Hindoliya DA. Experimental performance of new evaporative cooling pad materials. Sustain Cities Soc 2011;1(4):252–6.
[19] Khalajzadeh V, Farmahini-Farahani M, Heidarinejad G. A novel integrated system of ground heat exchanger and indirect evaporative cooler. Energ Buildings 2012;49:604–10.
[20] Riangvilaikul B, Kumar S. An experimental study of a novel dew point evaporative cooling system. Energ Buildings 2010;42(5):637–44.
[21] Khalid O, et al. Experimental analysis of an improved Maisotsenko cycle design under low velocity conditions. Appl Therm Eng 2016;95:288–95.
[22] Sohani A, Sayyaadi H. Thermal comfort based resources consumption and economic analysis of a two-stage direct-indirect evaporative cooler with diverse water to electricity tariff conditions. Energ Conver Manage 2018;172:248–64.
[23] Lin J, et al. Towards a thermodynamically favorable dew point evaporative cooler via optimization. Energ Conver Manage 2020;203:112224.
[24] Badiei A, et al. Can whole building energy models outperform numerical models, when forecasting performance of indirect evaporative cooling systems? Energ Conver Manage 2020;213:112886.
[25] Chen Q, et al. Simultaneous production of cooling and freshwater by an integrated indirect evaporative cooling and humidification-dehumidification desalination cycle. Energ Conver Manage 2020;221:113169.
[26] Farmahini Farahani M, Heidarinejad G, Delfani S. A two-stage system of nocturnal radiative and indirect evaporative cooling for conditions in Tehran. Energ Buildings 2010;42(11):2131–8.
[27] Shirmohammadi R, Gilani N. Effectiveness Enhancement and Performance Evaluation of Indirect-Direct Evaporative Cooling System for a wide Variety of Climates. Sustainable. Energy 2018.

[28] Farmahini-Farahani M, Delfani S, Esmaeelian J. Exergy analysis of evaporative cooling to select the optimum system in diverse climates. Energy 2012;40(1):250–7.
[29] Kloppers JC, Kröger DG. The Lewis factor and its influence on the performance prediction of wet-cooling towers. Int J Therm Sci 2005;44(9):879–84.
[30] Zalewski W, Gryglaszewski PA. Mathematical model of heat and mass transfer processes in evaporative fluid coolers. Chem Eng Process 1997;36(4):271–80.
[31] Maclaine-cross IL, Banks PJ. A general theory of wet surface heat exchangers and its application to regenerative evaporative cooling. J Heat Transfer 1981;103(3):579–85.
[32] Feltzin AE, Benton D. A more exact representation of cooling tower theory. Cooling Tower Instit J 1991;12(2):8–26.
[33] Sutherland JW. Analysis of mechanical-draught counterflow air/water cooling towers. J Heat Transfer 1983;105(3):576–83.